Proceeding of the 1st ICEENG conference, 24-26 March, 1998.

MILITARY TECHNICAL COLLEGE
CAIRO-EGYPT

ICEENG 98

FIRST INTERNATIONAL CONF. ON
ELECTRICAL ENGINEERING

A FRACTAL-BASED APPROACH FOR RADAR TARGET RECOGNITION

Abdallah M. Elramsisi, and Osama S. Elshehry
Air Force Reseach & Development Center, Air Force Information System Branch

Abstract- This paper presents a new approach for classifying radar targets through the fractal analysis of their radar echo. Radar target echo and clutter models have been generated from Rayleigh and Weibul distributions. oth target and clutter signatures have shown fractional Brownian motion behavior. The radar echo of a target varies basically according to radar target cross section (RCS) and more specifically according to the size, and geometric shape of the target. Those variations have been efficiently captured and abstracted in terms of average holder constant. Radar target echo and clutter have also been transformed into invariant symmetrized dot pattern (SDP) plot, where a correlation coefficient factor, R, has been computed. The two features, average holder constant and R have been presented to a multi-resolution neural network to classify seven types of aircraft in the presence of clutter. The multi-resolution neural net is composed of three sub-nets, each sub-net is a three-layered neural net with a back propagation learning algorithm. Conclusive classification results have been obtained and analyzed in terms of confusion matrix format.

Key words: Fractional Brownian motion, radar target echo, clutter, symmetrized dot pattern, average holder constant, radar cross section

1-Introduction

The main objective of this paper is two folds, the first is to provide a new estimation of a radar cross section (RCS) through the Fractal analysis and computation of average holder constant (AHC) for radar target echo, the second is to classify radar targets using a muki-resolution neural net classifier with two input features, the first is the AHC and the second is the correlation factor, R, of SDP plots of each target echo. The important properties of fractal signal models, which enable them to be modeled so simply, are self similarity and statistical invariance over wide ranges of scales. One of the most useful mathematical models for the random fractal signal has been the fractal Brownian motion (fBm) of Mandelbrot and Van Ness. It is an extension of the central concept of Brownian motion that has played an important role in both physics and mathematics [1]. A fractal Brownian function, $V_H(t), 0 < H < 1$, is a single valued function of one variable, t (usually time). When H is close to 0 the traces are roughest while as H approaches 1, traces are relatively smooth. H relates the typical change in V, $\Delta V = V(t2) - V(t1)$, to the time difference $\Delta t = t2 - t1$ by the simple scaling law [1]:

$$\Delta V \propto \Delta t^{H} \qquad (1)$$

whereas the self similar shapes repeat (statistically or exactly) under a magnification, the fBm traces repeat statistically only when the t and V direction are magnified by different amounts. If t is magnified by a factor r(t becomes rt), then V must be magnified by a factor r^H (V becomes $r^H V$). The variance of variations is proportional to the increment value as [1] :

$$\sigma^2(\Delta V) \propto (\Delta t)^{2H} \qquad (2)$$

The variations of a fBm $V_H(t_i) - V_H(t_{i-1})$ has a Gaussian distribution each with variance [1]:

$$\sigma^2 (VH(t_i) - VH(t_{i-1})) \propto (t_i - t_{i-1})^{2H} \quad (3)$$

then the standard deviation of the variations can be written as [1]:

$$\sigma\ (V_H(t_i) - V_H(t_{i-1})) \propto (t_i - t_{i-1})^{H} \quad (4)$$

this relation is known as T^H law where $T^H = (t_i - t_{i-1})^H$

The fractal dimension D, is a real value greater than the topological dimension E. The relationship between D, E, and the roughness measure H is given by: D = E+1-H. For one dimensional ,1-D, signal such as noise, E=1, D=2-H. For two dimensional, 2-D, signal, E=2, D=3-H, [1]. The fractal dimension is considered scale-, rotation-, and translation-invariant. A second fractal feature is the average holder constant (AHC) which is related to the fractal dimension (D) but is sensitive to the scale in predictable manners. Let T be the spacing of a sequence of points, and let $|\Delta V_i| = |V(t_i) - V(t_{i-1})|$. Then for a fBm $V_H(t)$, the local holder constant is given by :

$$\alpha_i = \frac{Log(|\Delta V_i|)}{Log(T)} \quad (5)$$

The AHC, for a fBm function $V_H(t)$ can be computed from (5) as follows, [2]:

$$\bar{\alpha} = \underset{i}{avg}(\alpha_i) = \underset{i}{avg}\left[\frac{Log(|\Delta V_i|)}{Log(T)}\right]. \quad (6)$$

Symmetrized dot pattern (SDP) is one of the most striking and colorful data display techniques which produces figures with the six fold symmetry. The clue is to convert data into a collection of dots which is reflected through mirror planes by a simple computer program. To implement the symmetrized dot pattern, starting with a digitized wave, the data is mapped in to a snowflake like pattern by comparing each pair of adjacent points, and plotting the result on a polar coordinate graph, and then reflecting the points through a mirror plane.. SDP plot is also considered to be scale-, rotation-, and shift-invariant, [2].

Radar target is described by an effective area called the radar cross section area ,RCS. It is the projected area of an equivalent sphere which would return the same echo signal as the target. An object exposed to an electromagnetic wave disperses incident energy in all direction. This distribution of energy in space is called scattering, and the object itself is often called the scatterer. The energy scattered back to the source of the wave, called (back scattering) constitutes the radar echo of the object. The intensity of the echo is described explicitly by the radar cross section (RCS) of the object. The formal definition of RCS is given by, [3]:

$$\varepsilon = \lim_{r \to \infty} 4\pi r^2 \frac{|E_S|^2}{|E_0|^2}. \quad (7)$$

where E_0 is the electric-field strength of the incident wave impinging on the target, E_S is the electric-field strength of the scattered wave at the radar, and r is typically taken to be the range from the radar to the target. The dependence of the RCS on r, and the need to form the limit, usually disappears [3,4].

From the study and analysis of the radar target echo, it has been found that they reflect statistical self similarity . This feature invited us to study the fBm behavior of the radar echo signals for different target's

Radar echo signals for different targets (bombers, fighters,...) have been simulated as a Rayleigh distribution according to their RCS values. Clutter signals have also been simulated as a Weibul distribution [3,4]. The fBm behavior of both radar target echo signals and clutters have been shown through the verification of the T^{4} law in one hand and the normal distribution of the variation histogram on the other hand [5]. Proposed average values of RCS's, in square meter, for different types of targets are shown in table 1, [6].

Table 1 : The Average RCS Of Targets

Broad Class Of Targets	verage RCS
Single engine fighters	1
Small fighters	2 to 3
Large fighters	5 to 6
Small bombers	10
Medium bombers	40
Large bombers	80
Cargo	>= 100

2-Radar Echo Generation

Although there are few cases in which the RCS values are constant, it will generally vary considerably for each target as the change of the aspect angle of the target shape, and the radar frequency. These changes force us to use statistical methods to describe the radar target [3,4]. In his classical paper on target modeling, Peter Swerling established four statistical models for radar targets [4]. The Swerling model case1 is the fluctuating target most frequently used for calculation. It is a description of a collection of many independently moving scatters (Rayleigh amplitude distribution).

2-1 Target Generation

The radar echo of the target takes the form of Rayleigh distribution in Swerling case1. The Rayleigh probability density (pdf) and the commutative distribution function (cdf) are given by, [3,4] :

$$f(x) = (1/\bar{x}) * \exp[-(x/\bar{x})]. \quad (3)$$

$$F(x) = 1 - \exp[-(x/\bar{x})] \quad (4)$$

where x is the Rayleigh random variable, $x > 0$ and $\bar{x}$ denotes the mean RCS value. A Rayleigh random variable can be generated as follows :

Set F(x)=U. Solve for x in terms of $\bar{x}$. Then x can be written as :

$$x = -Ln(1-U)\bar{x} \quad (5)$$

where U is a uniform random number. Fig. 1 depicts a generated Rayleigh random variable for target echo with RCS = $10\,m^2$.

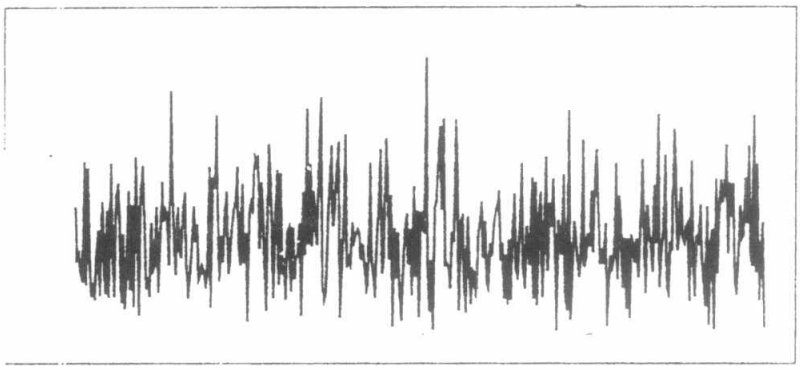

Fig. 1 : generated echo for target with RCS=10 m^2

2-2 Clutter Generation

According to Swerling - case1, some clutter take the form of Weibul distribution. The pdf and cdf of the Weibul distribution in its general form is given by [3,4] :

$$f(x) = \begin{cases} bx^{-b}x^{b-1}e^{-(x/a)^b}, & x > 0 \\ 0 & x = 0 \end{cases} \qquad (11)$$

$$F(x) = [1 - \exp(-x/a)^b] \qquad (12)$$

where a, b>0 are the scale and shape parameters respectively. A random Weibull variable can be generated as follows :

Set $F(x) = U$, then x can be written as:

$$x = [-Ln(1-U)]^{1/b} a \qquad (13)$$

The pdf and cdf for clutter can be described as:

$$f(x) = \{Ln(2)b(x)^{b-1} \exp(-(\ln(2))x^b\} \qquad (14)$$

$$F(x) = 1 - \exp(-Ln(2)x^b), \qquad (15)$$

and the Weibull random variable, x can be written as follows :

$$x = (-\frac{Ln(1-U)}{Ln(2)})^{(1/b)}. \qquad (16)$$

Fig. 2 depicts a generated Weibull random variable for clutter with b=0.3

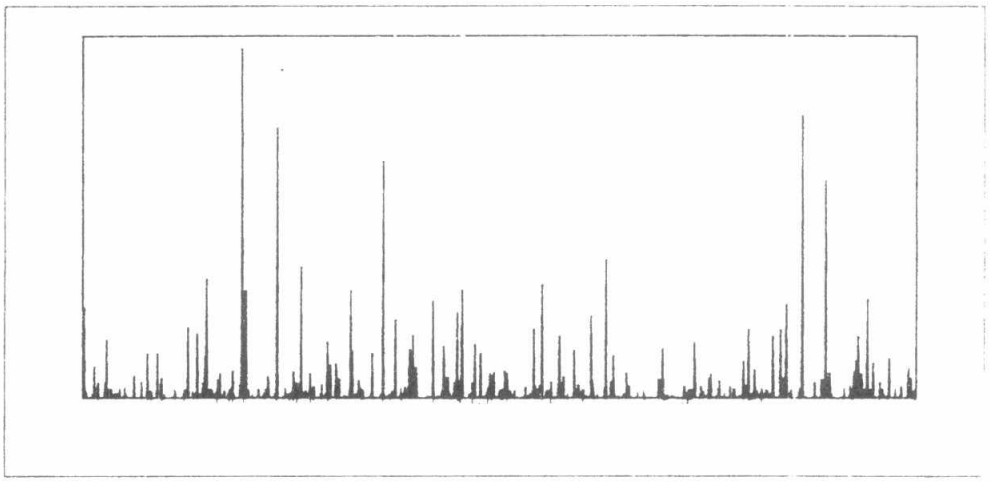

Fig. 2: Generated echo for clutter with b=0.3

The verification of the fBm behavior for radar target echo and clutters are shown in fig (3 to 6). Where the T^H plots reflect linear relation, and the variation histogram depicts Gaussian distribution.

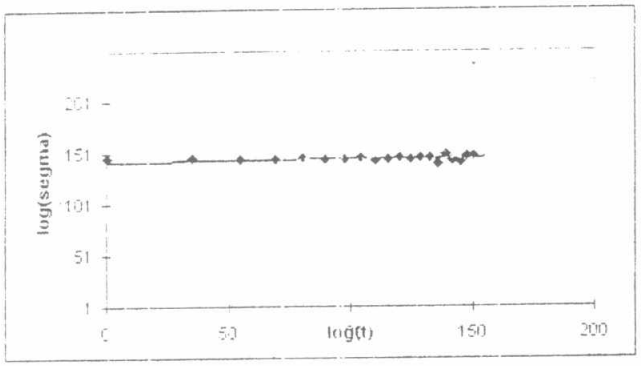

Fig. 3. T^H verification for target with RCS=10 meter square, RMSE=0.59

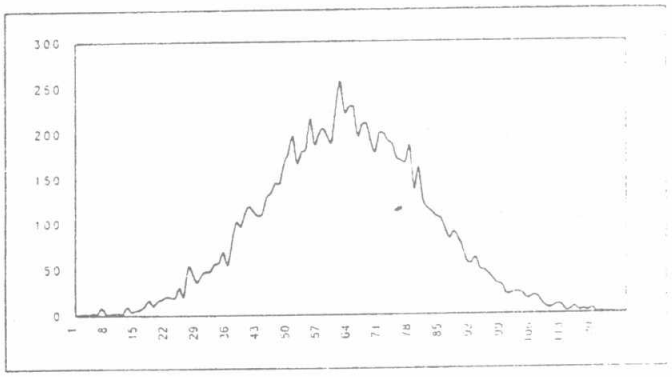

Fig. 4. Histogram for target with RCS=10.

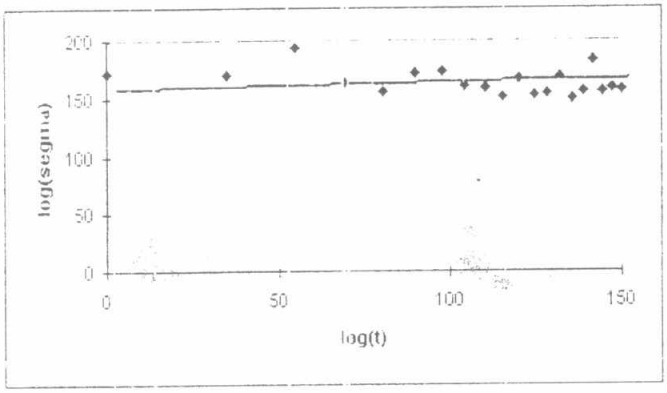

Fig. 5. T^H verification for clutter with b=0.4,RMSE=2.49.

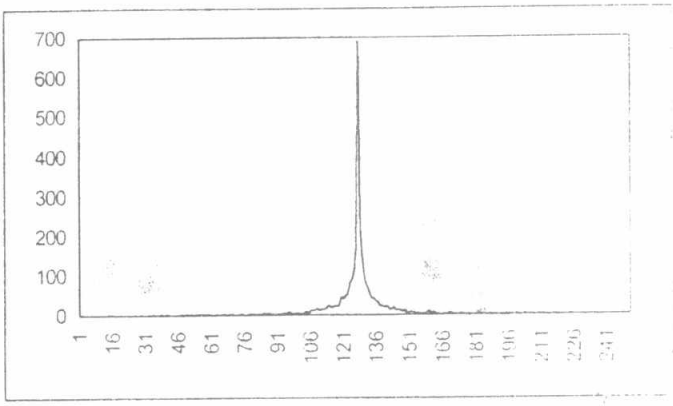

Fig. 6. Histogram verification for clutter with b=0.3.

3-RCS Estimation

A main focus of this research effort is to provide an estimate of radar target cross section through fractal analysis of radar echo. The average holder constant of the fBm traces provides an important information about the nature of the target, and more specifically size and shape [5.6.7]. The AHC has been computed for 120 radar targets and clutters of different RCS's. For 100 generations of each target and clutter, the region of the curve containing RCS values of targets of interest has been magnified as shown in fig. The RCS estimate can be abstracted in terms of 5th order polynomial of the following form :

$$RCS = 0.006 * (AHC)^5 - 0.0467 * (AHC)^4 - 0.0327 * (AHC)^3 + 0.457 * (AHC)^2 + 1.9514 * AHC - 1.9654 \quad (1)$$

The proposed RCS estimate has been successfully tested and validated over 100 target generations. The proposed RCS estimation method has achieved 5 % error percentage and 8.26 root mean square error rate between input RCS and estimated one.

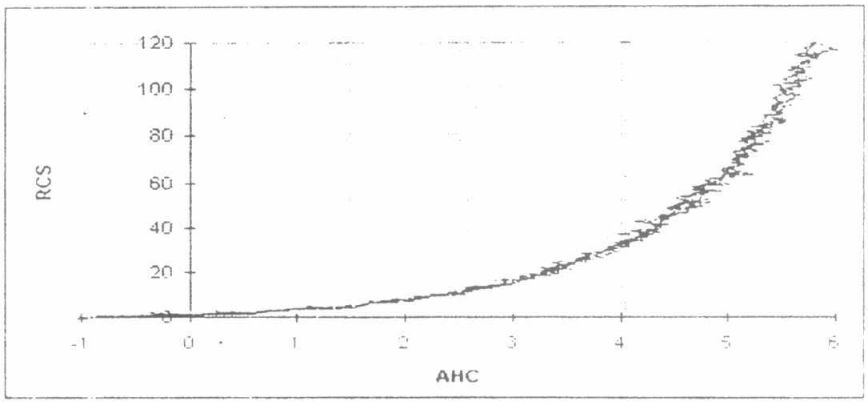

Fig. 7 : The relation between AHC and RCS (multiple running)

4 -SDP Plots For Targets And Clutters

SDP plots for targets of different RCS's and clutters of different b parameter are ploted in Fig.8 and Fig.9 respectively [2,7]. The SDP patterns have been plotted using 1000 points for each echo. A correlation coefficient R for each SDP plot is computed as the number. of displayed points divided by the total number. of points according to screen resolution. As the correlation among the points becomes lower, R values become higher and vice-versa. SDP patterns provide a qualitative and quantitative measures of target types in terms of SDP plot display, and the correlation coefficient, R. It can be noticed that clutters have lower correlation coefficient, R, and as b parameter gets higher, SDP plots for clutters approach SDP plots for target.

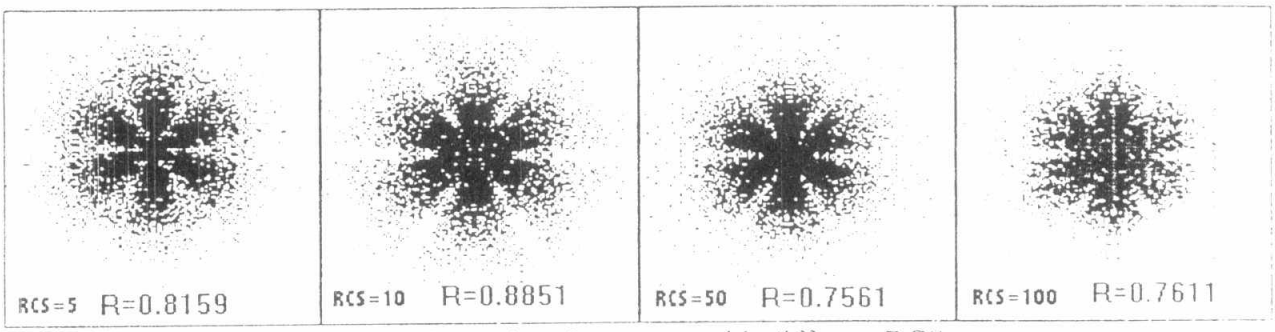

Fig. 8: SDP plots for targets with different RCS

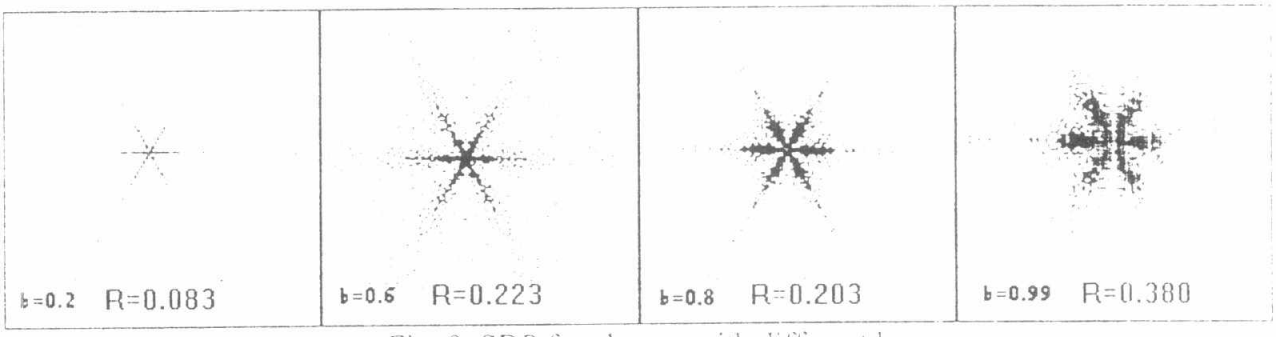

Fig. 9: SDP for clutters with different b

5-Neural Net Classifier

The block diagram of the proposed multi-resolution neural net classification scheme is shown in Fig. 10. The first layer, the general class subnet, classifies input samples to four major classes: cargo, bombers, fighters, and background clutter. The second layer consists of two neural sub-nets. The first one is used for classifying specific fighter types (large fighters as F-15, middle fighter as F-16, small fighter as Mig21,). The second subnet is used for classifying specific bomber types(large bomber, middle bomber, small bomber). Each subnet (bomber, fighter) is activated by an enable input from the general class subnet where the two input features (AHC, R) are available as input for the activated neural subnet. Fig. 11 (a, b, c) depicts the three neural subnet architectures. Each subnet is composed of three layers, and adopts a back propagation learning algorithm [8]. Fig.12 depicts graphical representation of the feature space, where the back ground clutter class occupies the bottom area, and the other seven classes of targets: small fighter, middle fighter, large fighter, small bomber, middle bomber, large bomber, and cargo occupy the upper area of the graph from left to right respectively.

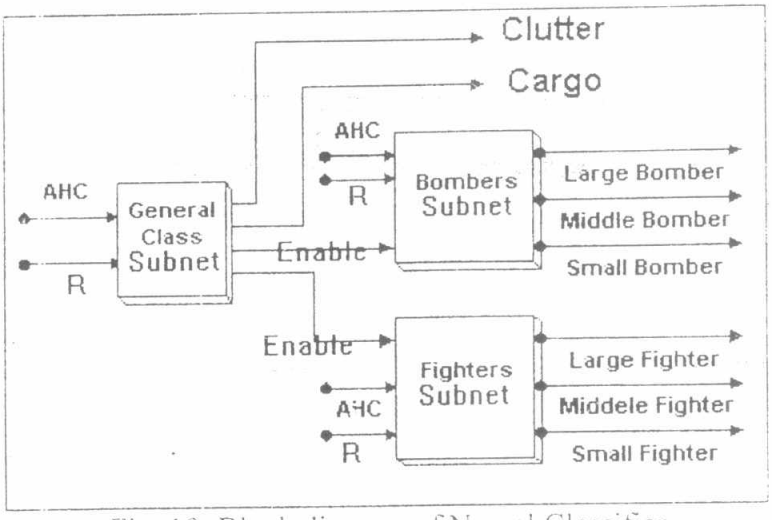

Fig. 10: Block diagram of Neural Classifier

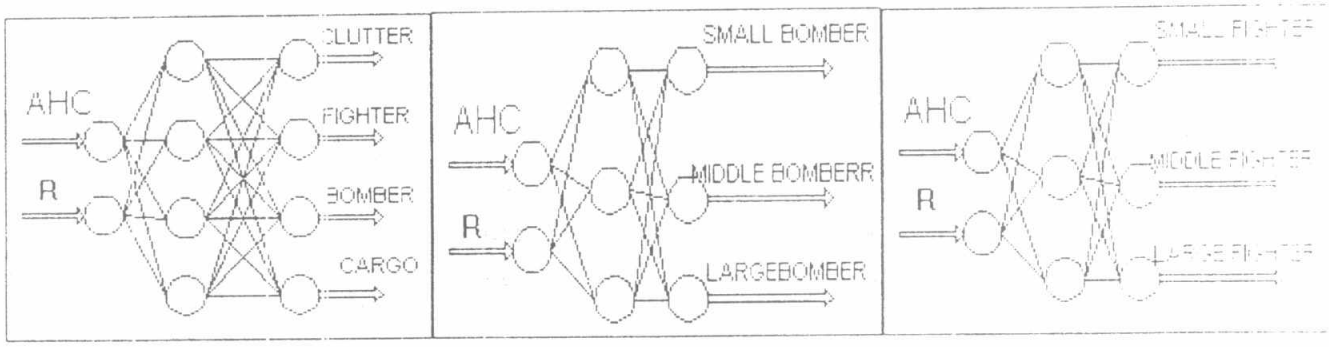

Fig. 11.a. General Class Subnet Fig.11.b Bombers Subnet Fig. 11.c. Fighters Subnet

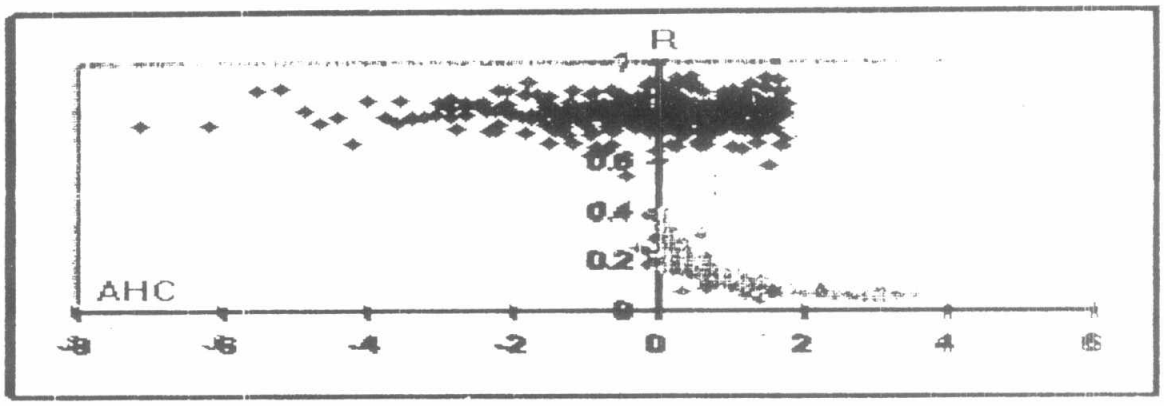

Fig. 12. Graphical Representation Of Feature Space

The performance of the proposed multi-resolution classification scheme has been tested and analyzed. Test results are summarized in the confusion matrix shown in table 4, where samples of each class have been presented to the classifier 100 times [7]. The average value of the percentage of correct recognition is 88%. The recognition rate for each class is computed as the number of times the classifier outputs a specific class with respect to the 100 presentations. For example, the classifier outputs large fighter 131 times.

Table4 : Confusion matrix of the classifier

	Small Fighter	Middle Fighter	Large Fighter	Small Bomber	Middle Bomber	Large Bomber	Cargo	Clutter	Recognition Rate
Small Fighter	81								0.81
Middle Fighter	18	68							0.86
Large Fighter		31	100						1.3
Small Bomber				89					0.89
Middle Bomber				11	68				0.79
Large Bomber					32	100			1.32
Cargo							100		1
Clutter								100%	1
unclassified	1	1							0.02
Correct Recognition %	81%	68%	100%	89%	68%	100%	100%	100%	

6. Conclusion

The proposed approach presents a new reliable method for radar target classification based on the fractal estimation of the radar cross section. The average holder constant for each signal has been used to provide an estimate for target RCS. The correlation factor, R, of SDP plots along with RCS estimates for targets and clutters have been used to classify samples from eight target classes. The proposed scheme can be used in a wide spectrum of military applications, especially reconnaissance and early warning radar systems.

References

[1] M. F. Barnsely, R. L. Devaey," The Science Of Fractal Images," *Spring-Verlage, NY, 1998.*

[2] Clifford A. Pickover, " Computers, Pattern, Chaos and Beauty," ST. Martin's Press, NY, 1990.

[3] Skolnik M.," Introduction To Radar System," *McGraw-Hill, 1980.*

[4] Peter Swerling, "Probability Of Detection For Fluctuating Target," *IRE Trans. On Information Theory, April 1960, pp. 296-307.*

[5] James M. Keller, Richard M. Crownver, and Robert Yu Chen, " Characteristics Of Natural Scenes Related To The Fractal Dimension", *IEEE Transactions On Pattern Analysis And Machine Intelligence, Vol. PAMI-9, No 5, September 1987.*

[6] Stuart M. Lee, editor, " Stealth Low Observable Composite Aireraft", International Encyclopedia of Composites, Vol. 6, pp. 404 - 420, VCH, NY.

[7] A. M. Elramsisi, I. A. Ismail, B. Ahmed Baz," On The Classification Of partially - occluced Fractal Images," *Proceeding of the fourth International Conference On Artificial Intelligence Applications, ICAIA, pp. 137 - 150, Cairo, Egypt, Jan 16-19, 1996.*

[8] R. Lippman, "An Introduction To Computing With Neural Nets", *IEEE, ASSP Magazine, pp. 4-22, April 1987.*